

STRUCTURAL CONDITION ASSESSMENT OF COMPOSITES USING IMAGE PROCESSING AND WAVELET ANALYSIS

Andrzej Katunin^{1a}, Angelika Wronkowicz^{1b}

¹Institute of Fundamentals of Machinery Design, Silesian University of Technology

^aandrzej.katunin@polsl.pl, ^bangelika.wronkowicz@polsl.pl

Summary

The paper describes a method of the identification of cracks basing on in-plane deflection profiles of structural elements, which is based on vision data acquisition, intelligent image processing procedures and wavelet analysis. The experimental studies were carried out on composite preloaded beams with single and multiple artificial cracks with variable depths. The preloading of beams allows for detection and localization of breathing cracks using the proposed method. An Application of wavelet transform of the deflection profiles obtained during image processing makes possible the identification of cracks basing on even the smallest irregularities of the deflection curvatures. Such a non-contact method provides an efficient condition assessment of beam-like structures and could be used as a continuous condition monitoring tool as well, which is much more cost-efficient solution than the presently used strain gauge-based measurement systems.

Keywords: composite structures, condition assessment, image processing, wavelet analysis

STRUKTURALNA OCENA STANU KOMPOZYTÓW Z WYKORZYSTANIEM PRZETWARZANIA OBRAZÓW I ANALIZY FALKOWEJ

Streszczenie

W artykule opisano metodę identyfikacji pęknięć na podstawie profili ugięcia elementów strukturalnych, która jest oparta na akwizycji danych wizyjnych, inteligentnym przetwarzaniu obrazów oraz analizie falkowej. Próby eksperymentalne były przeprowadzone na wstępnie obciążonych belkach kompozytowych ze sztucznie wprowadzonymi pojedynczymi i wielokrotnymi pęknięciami o różnych głębokościach. Wstępne obciążenie belek pozwala na detekcję i lokalizację „oddychających” pęknięć z wykorzystaniem proponowanej metody. Zastosowanie transformacji falkowej do profili ugięcia otrzymanych podczas przetwarzania obrazów umożliwia identyfikację pęknięć na podstawie nawet najmniejszych nieregularności krzywizn ugięcia. Taka bezkontaktowa metoda zapewnia efektywną ocenę stanu struktur belko-podobnych i może być stosowana jako narzędzie ciągłego monitorowania stanu, co jest znacznie bardziej opłacalnym rozwiązaniem, niż aktualnie stosowane systemy pomiarowe oparte na tensometrii.

Słowa kluczowe: struktury kompozytowe, ocena stanu, przetwarzanie obrazów, analiza falkowa

1. INTRODUCTION

The mechanical and civil engineering constructions are subjected to the degradation processes occurred during their operation. It requires their condition assessment and monitoring in order to detect and localize the damages in possible early stages of development for

prevention of the breakdown of such constructions and eventual catastrophic consequences. The modern condition monitoring systems should fulfill the following criteria: they should be sensitive for even the smallest damages occurred in the investigated objects, should not

influence on the structure, should provide detection and precise localization of arbitrary number of occurred damages, and should be low-cost. The methods of condition monitoring of structures and constructions can be divided into two categories: damage assessment based on dynamic response (e.g. modal analysis, infrared thermography) and the methods based on the static testing data (e.g. analysis of static displacements and curvatures, static strain) [1-4].

The methods, which are based on dynamic testing data, often reveal better sensitivity to the damage presence and better accuracy of their localization in comparison with methods based on the static testing data. This is because of analyzing of multiple modal shapes during application of vibration-based methods, which contain useful diagnostic information [5]. However, for the dynamic testing of structures and constructions expensive measurement equipment is necessary, e.g. laser vibrometers, or manufacturing of expensive structures with embedded measurement devices, e.g. structures with piezoelectric transducers or fiber Bragg gratings, need to be performed.

The second group of the testing methods is less sensitive to the occurred damages than the dynamic testing methods, however such methods could be much more cost-efficient than the dynamic ones. One of the promising approaches applied in the structural condition assessment is the application of vision-based measurements and further processing of achieved vision data in order to detect and identify the damage and its position. Such an approach provides a possibility of non-contact assessment at long distances (thus the large structures could be analyzed as well), however it requires heavier processing algorithms and the accuracy of such methods of damage identification is dependent on the resolution properties of the registered vision data [6,7]. Numerous studies concerned with an application of vision-based techniques for structural condition assessment were used for monitoring of bridges, e.g. Morlier et al. [8] analyzed the modal shapes of the vibrating bridge in order to identify the structural damages. Other studies present the analysis of small beam-like structural elements and their diagnosing using the vision methods. The authors of [9] presented an interesting approach of two-camera measurements with smart markers detection for the condition assessment purposes.

Several authors used the wavelet analysis for the acquired vision data in order to detect and localize the damages, e.g. Patsias and Staszewski [10] applied the wavelet-based approach for the edge detection problem, Poudel et al. [11] used the wavelet-based method for the structural damage detection of modal shapes, while Pakrashi et al. [12,13] applied the wavelet-kurtosis method for damage identification in preloaded beams. Such a popularity of the wavelet analysis is because of

its great sensitivity to the non-monotonocities of the analyzed signal.

The wavelet analysis is successfully applied in the structural diagnostics problems based on the displacements measurements. Several studies of the first author [5,14-16] proved the effectiveness of such a methodology. However, following the results obtained by Rucka and Wilde [17], the application of the wavelet analysis to the displacement data of static deflection profiles seems to be ineffective, the lower limit of the crack depth detectable by the wavelet-based method proposed by the authors was about 50% of total thickness of the analyzed structure.

The main goal of this paper is to present an automated method based on image processing with using a segmentation procedure and intelligent selection of the region of interest with complex fractional B-spline wavelet-based postprocessing of the deflection profiles of beams. The effectiveness of an application of such wavelets for the analysis was justified in the previous studies [16]. The order of the wavelet applied to the analysis was selected during the direct search optimization. The influence of damage position, crack depth and the magnitude of deflection on the accuracy of detection and localization were analyzed. The problems of the application of the proposed method were also discussed.

2. THE METHODOLOGY

The damage identification procedure consisted of the following steps. At the first stage, the experimental deflection profiles of the tested beams with artificial damages were registered using camera-based optical measurement technique. Then, the obtained images were processed using intelligent pattern recognition in order to identify the deflected beam on the image and extract the deflection profile. Finally, the wavelet analysis of the extracted profiles was performed in order to detect and localize the damages. Further, the damage identification procedure was described in detail.

2.1 SPECIMENS AND EXPERIMENTAL SETUP

The laminated beams made of glass cloth reinforced epoxy resin produced by Izo-Erg Sp. z o.o., Gliwice (symbol EP GC 201) were prepared for the tests. The mechanical properties of the material can be found in [18]. The dimensions of the specimens were as follows: length l of 320 mm, width w of 10 mm and thickness h of 2.5 mm. The specimens were clamped on the one side and loaded on the opposite one with different masses (see Fig.1). Five loading masses were considered during the tests: 36.9, 153.8, 231.8, 305.5 and 378.8 g.

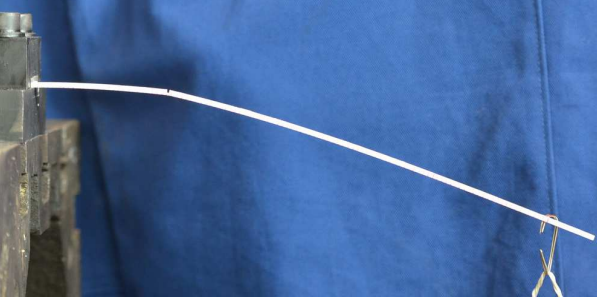


Fig. 1. Exemplary view of the loaded specimen

Due to the clamping and loading connection with the specimen the length of it was shortened to the working length L of 280 mm. The damages were artificially made using a saw. Three cases of depths d of damages were considered: 0.5 mm, 1 mm and 1.5 mm, which coincides to the d/h ratio as follows: 20%, 40% and 60%, respectively. During the tests three cases of number of damages were investigated: the specimens with single, double and triple cracks. Each of these cases consisted of the subcases with various locations of these cracks. The full specification of the considered cases with the cracks positions was listed in Table 1.

Table 1. Locations and depths of the considered damages

Case	No. of cracks	Location, -	Depths, mm		
1	Single	$\frac{1}{4} L$	0.5		
2			1		
3			1.5		
4		$\frac{1}{2} L$	0.5		
5			1		
6			1.5		
7	Double	$\frac{1}{4} L$,	0.5, 0.5		
8			$\frac{1}{2} L$	1, 0.5	
9				0.5, 1	
10				1, 1	
11		$\frac{1}{2} L$,	$\frac{1}{4} L$,	1.5, 0.5	
12			$\frac{3}{4} L$	0.5, 1.5	
13			$\frac{1}{4} L$,	$\frac{1}{2} L$,	0.5, 0.5
14				$\frac{3}{4} L$	1, 0.5
15				0.5, 1	
16				1, 1	
17		Triple	$\frac{1}{4} L$,	1.5, 0.5	
18				$\frac{1}{2} L$,	0.5, 1.5
19	$\frac{1}{2} L$,		$\frac{3}{4} L$	0.5, 0.5, 0.5	
20				0.5, 1, 0.5	
21				0.5, 1, 1	
22				1, 0.5, 0.5	
23		1, 1, 0.5			
24		1, 1, 1			

2.2 IMAGE ACQUISITION AND PROCESSING

The surface of observation of each specimen was painted white in order to ensure the better contrast with other elements visible on the images. The acquisition was performed using digital camera Nikon® D7000 located on the distance of 1 m from the observed specimen. A size of obtained photographs was about 4 Mpx. The photographs were saved in RGB (red, green, blue) color space.

In order to extract the deflection profiles of the specimens the following transformations were applied. Firstly, all of the RGB values were normalized to the unitary range and the empirically determined threshold of 0.9 was applied in order to separate the white region of the specimen (Fig.2a). Afterwards, the singleton dimensions from the RGB triplets were removed, what allows for image binarization (Fig.2b). Then, the boundary tracing algorithm was applied in order to select the non-zero-value regions on the binarized image (Fig.2c).

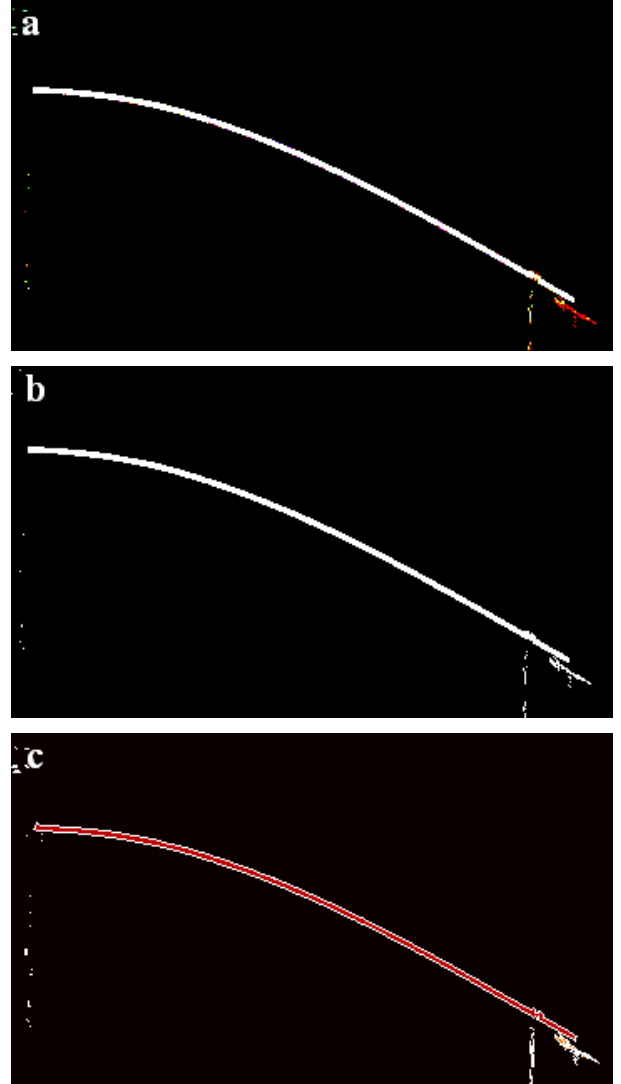


Fig. 2. Image processing procedures

After the regions detection the algorithm selected the area concerned with the investigated specimen using its geometrical properties. The boundary of the selected region was transformed into a set of points with planar coordinates and the deflection curve of the top of the specimen was selected to further analysis (Fig.3). The direction of deflection was inverted due to the image processing procedure.

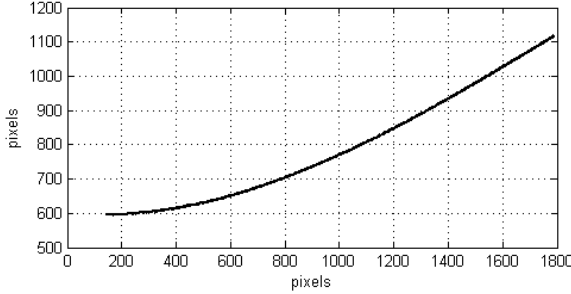


Fig. 3. Deflection curve after the image processing procedures

Considering a fact that during the experimental studies large deflections of beams were observed the consideration of horizontal projections of the profiles could not be analyzed because of shortening the profile. Therefore, it is necessary to transform obtained profiles in order to assure proper localization of the cracks. For this purpose the following operations were applied. Firstly, the profiles were divided into 20 sections and each of them was interpolated using polynomial function of the third degree. The degree of polynomial function was selected according to the power of three in the formula for the deflection function of a cantilever beam [19]. Then, the length of the interpolated section was determined and the ratio between this length and its horizontal projection was calculated. The sections of the original profiles were multiplied by the calculated ratio, different for each considered section. The transformed sections were then joined with appropriate shifting of their ends in order to assure the monotonicity of the transformed profile.

2.3 WAVELET ANALYSIS

In order to detect and localize the damages based on obtained deflection curves the wavelet transform was applied. Following to the previous findings [16] the complex fractional B-spline wavelets were used during the analysis. Their effectiveness with respect to other wavelets was conducted by several authors, e.g. in [20].

The complex fractional B-spline wavelets were developed by Unser and his scientific team. The fundamentals of this wavelet family can be found in [21], which were extended in several further studies [22,23].

The general order fractional B-spline scaling β_τ^α and wavelet ψ_τ^α functions are presented by the following expressions [21]:

$$\beta_\tau^\alpha(x) = \sum_{k=0}^{\infty} (-1)^k \binom{\alpha+1}{k-\tau} \rho_\tau^\alpha(x-k), \quad (1)$$

where $\alpha \in \mathbf{R}$ is the order of a B-spline, $\tau \in \mathbf{R}$ is the shift parameter and ρ_τ^α is the function of the following form:

$$\rho_\tau^\alpha(x) = -\frac{\cos \pi \tau}{2\Gamma(\alpha+1)\sin(\pi\alpha/2)} |x|^\alpha - \frac{\sin \pi \tau}{2\Gamma(\alpha+1)\cos(\pi\alpha/2)} |x|^\alpha \operatorname{sgn}(x), \quad (2)$$

where $\Gamma(\alpha+1)$ is the Euler gamma-function, which allows for the fractional factorization;

$$\psi_\tau^\alpha\left(\frac{x}{2}\right) = \sum_{k \in \mathbf{Z}} \frac{(-1)^k}{2^\alpha} \sum_{l \in \mathbf{Z}} \binom{\alpha+1}{l} \cdot \beta_0^{2\alpha+1}(l+k-1) \beta_\tau^\alpha(x-k). \quad (3)$$

The process of the wavelet-based signal decomposition could be considered as a filtering procedure using a set of high-pass and low-pass filters. The high-pass (scaling) filter could be described basing on its pulse response [24] in the form:

$$H_\tau^\alpha(e^{j\omega}) = 2^{-\alpha} \frac{(1 + e^{j\omega})^{\frac{1}{2}(\alpha+1)-\tau}}{(1 + e^{-j\omega})^{\frac{1}{2}(\alpha+1)+\tau}}, \quad (4)$$

while the low-pass (wavelet) filter is defined similarly in the form:

$$G_\tau^\alpha(e^{j\omega}) = -e^{-j\omega} H_\tau^\alpha(-e^{-j\omega}) A^\alpha(-e^{j\omega}), \quad (5)$$

where

$$A^\alpha(e^{j\omega}) = \sum_{k \in \mathbf{Z}} \beta_\tau^{2\alpha+1}(k) e^{-j\omega k}. \quad (6)$$

The proposed algorithm of the extraction of non-monotonocities of beam profiles is based on their single-level decomposition. After the decomposition the absolute values D of the obtained sets of details coefficients were calculated for clarity of presentation of results.

In order to select a suitable order of wavelet and scaling functions for the analysis the direct search algorithm was applied. Note that in the following case the causal B-spline wavelets were applied, i.e. the shift factor is in dependence of the order of the mentioned functions following the next relation: $\tau = (\alpha + 1)/2$. The variability limits of α were as follows: $0 \leq \alpha \leq 20$ with a step of 0.01. The selection of α was performed on the case 1 from Table 1. The resulted value of α equaled 3.01 was applied for further studies.

3. TESTS AND ANALYZES

RESULTS OF THE CRACKS DETECTION AND LOCALIZATION

The tests were carried out following the procedure described in the section 2. Exemplary results of the damage detection and localization for single, double and triple cracks were presented in Fig.4.

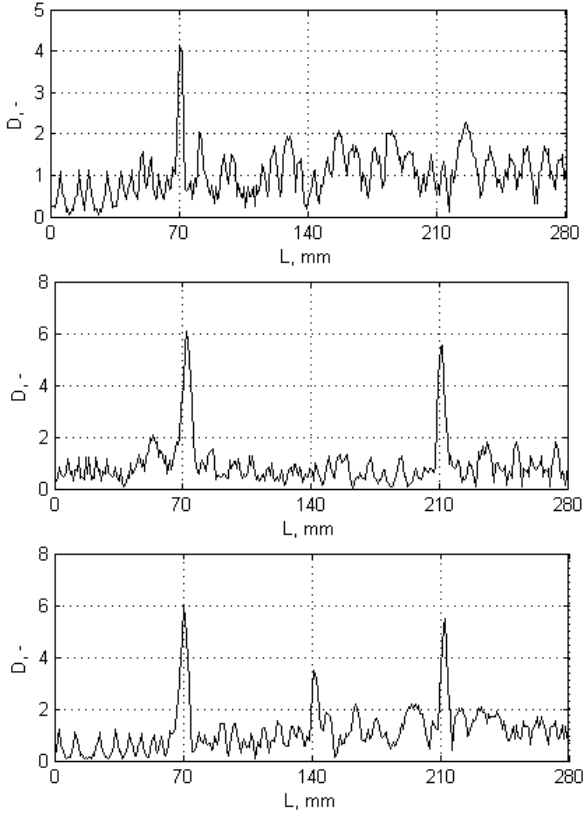


Fig. 4. Exemplary results of detection and localization of single, double and triple cracks

As it could be noticed all of the cracks in the presented cases were well detected and localized with high accuracy.

Then, the influence of the deflection magnitude and cracks depths on the detectability of the damages and its localization were investigated. Analyzing the results of cracks detection and localization the following measure of detectability ϵ was used: the peak values of D -coefficients for each detected crack were divided by the median value of the whole set of D -coefficients. The ratio between locations of detected cracks and their real locations was used as a measure of localization accuracy δ . The exemplary results of the analysis of influence of deflection magnitude for the case 5 (Table 1) were presented in Fig.5.

Results show that the increasing deflection of the structure influences negatively on the detectability of cracks, i.e. during the first stage of loading the crack was well detectable and localized. However, during the next loading stages the localization peak decreased with

respect to the median value of the whole set of D -coefficients (Table 2). Moreover, in the last stage of loading (Fig.5) the additional peak was detected, which was probably resulted from the detection of both sides of a crack. The localization results also varied slightly with respect from the original location of a crack.

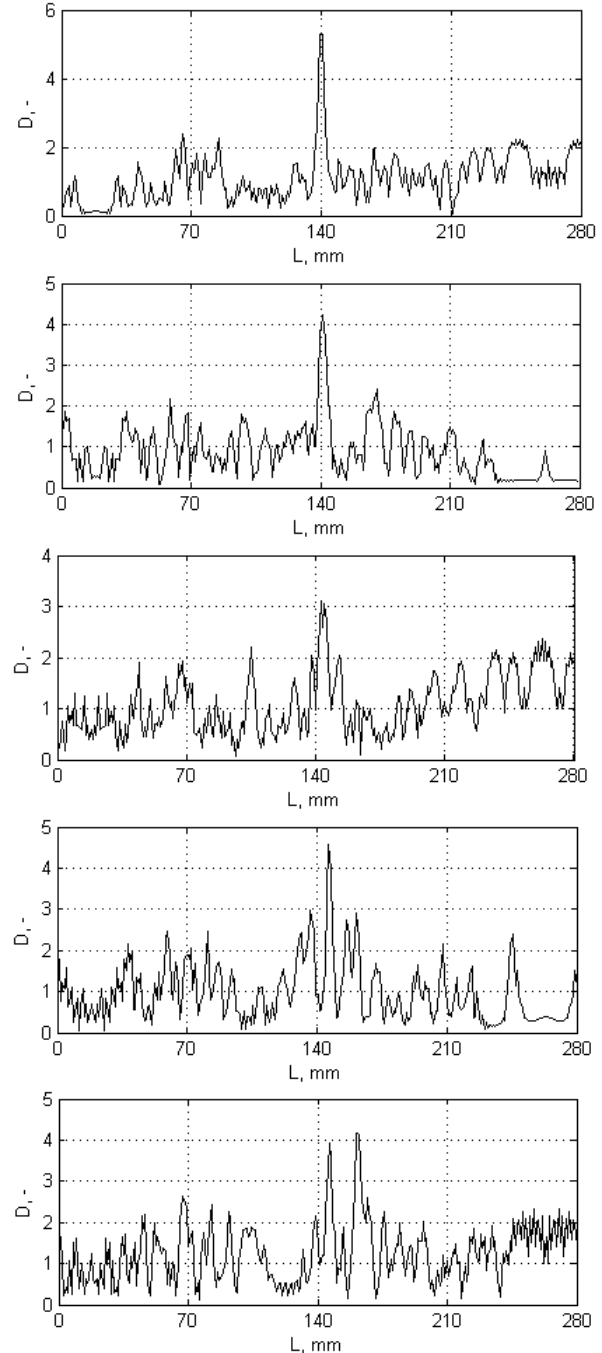


Fig. 5. Exemplary results of detection and localization of a single crack of a beam with five stages of loading

Table 2. Accuracy of a crack detection and localization

Loading stage	ϵ , -	δ , %
1 (36.9 g)	5.2088	0.1742
2 (153.8 g)	5.3255	0.6993
3 (231.8 g)	3.1024	1.0345
4 (305.5 g)	5.6328	2.0833
5 (378.8 g)	3.4939	2.2491

Next, the influence of the cracks depths and positions on the detectability and localization accuracy was analyzed. For the analysis of crack depth the cases with double cracks (8÷12) with loading stage of 2 were selected. Obtained results were presented in Fig.6.

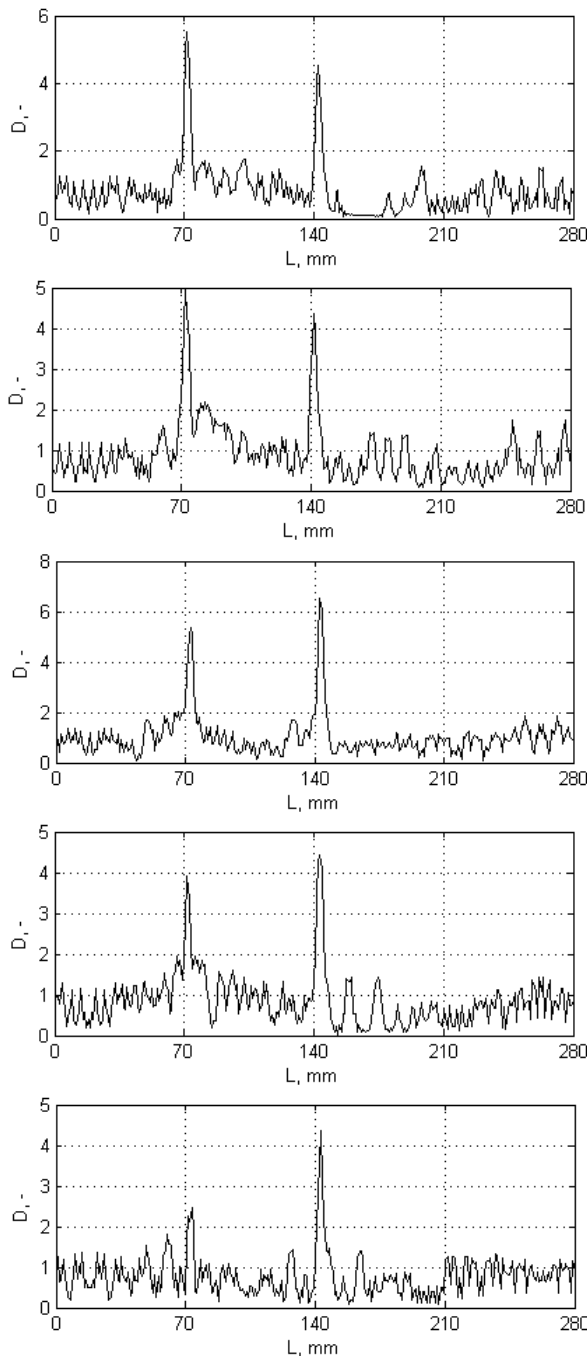


Fig. 6. Results for the analyzed cases of determination of influence of cracks depths on their detectability

Considering the obtained results presented in Fig.6 with the cracks depths following Table 1 it could be stated that cracks with various depths were well detected and localized, however the dependence between the crack depth and the magnitude of the D -coefficients in the selected locations was not observed.

The last issue investigated in this study concerned with the localization accuracy of the multiple-cracked beams. For this purpose it was suitable to select the cases with triple cracks. Considering a fact that the better results were obtained for the damaged beams with low loadings the results of analysis were presented for the first and second loading stages (see Table 3). The numbering of cracks in the beams was assumed from the clamped side. Selected results for the cases corresponded with Table 3 were presented in Fig.7.

Table 3. Localization accuracy for the triple-cracked beams

Case no.	Loading stage	δ , %		
		Crack no.		
		1	2	3
20	1	0.42	1.53	1.61
	2	0.43	1.20	1.63
21	1	0.42	0.51	0.93
	2	0.60	0.85	1.45
22	1	0.00	0.34	0.68
	2	0.42	1.19	0.59
23	1	0.59	0.51	0.76
	2	0.85	1.02	1.19
24	1	0.34	0.34	0.34
	2	0.60	1.19	0.77
25	1	0.59	1.51	–
	2	0.50	0.00	1.51
26	1	0.93	0.84	0.76
	2	0.68	1.01	0.68

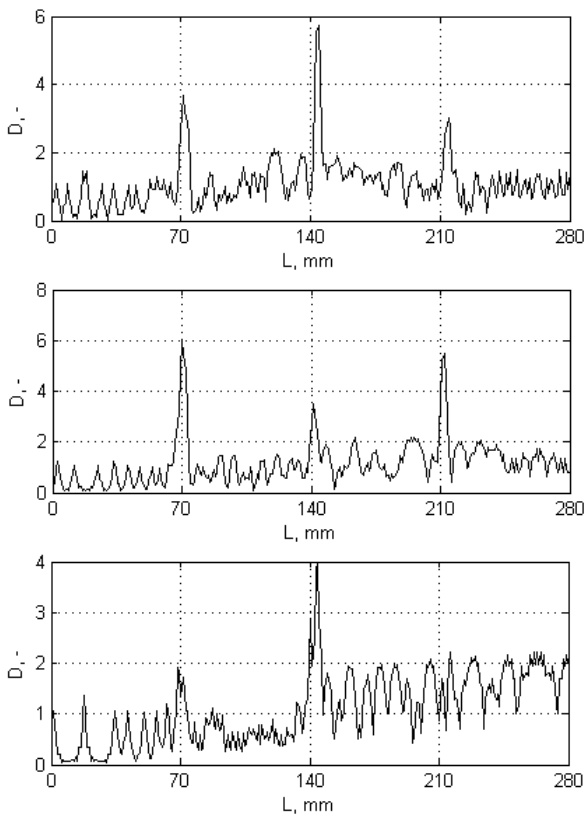


Fig. 7. Results for the cases 20, 22 and 25 under the first stage of loading

The cracks were precisely localized, i.e. the difference between real and localized positions of cracks for the triple-cracked beams was not exceeded 2%. It was observed that for the most analyzed cases with multiple cracks there is a tendency of shifting the localized position from original ones during the increase of distance

The research project was financed by the National Science Centre (Poland) granted according the decision no. DEC-2011/03/N/ST8/06205. The authors would like to acknowledge Dr. Marek Wyleźół and Ms. Karmena Serzysko for the assistance during carrying out the experimental studies.

References

1. Gu M., Xu Y.L., Chen L.Z., Xiang H.F.: Fatigue life estimation of steel girder of Yangpu cable-stayed bridge due to buffeting. "Journal of Wind Engineering and Industrial Aerodynamics" 1999, Vol. 80, p. 383 - 400.
2. Chen X.-Z., Zhu H.-P., Chen C.-Y.: Structural damage identification using test static data based on grey system theory. "Journal of Zhejiang University Science" 2005, Vol. 6A, p. 790 - 796.
3. Kohut P., Holak K., Dworakowski Z., Uhl T.: Vision data employed for crack detection and localization. "Diagnostyka – Applied Structural Health, Usage and Condition Monitoring" 2012, Vol. 63, p. 35 - 41.
4. Reynolds P.: Dynamic testing and monitoring of civil engineering structures. "Experimental Techniques" 2008, Vol. 32, p. 54 - 57.
5. Katunin A.: Damage identification in composite plates using two-dimensional B-spline wavelets. "Mechanical Systems and Signal Processing" 2011, Vol. 25, p. 3153 - 3167.
6. Stephen G.A., Brownjohn J.M.W., Taylor C.A.: Measurements of static and dynamic displacement from visual monitoring of the Humber bridge. "Engineering Structures" 1993, Vol. 15, p. 197 - 208.
7. Caetano E., Silva S., Bateira J.: A vision system for vibration monitoring of civil engineering structures. "Experimental Techniques" 2011, 4, Vol. 35, p. 74 - 82.

from the clamped side. This phenomenon is caused by increasing curvature of the deflected beam as well as inaccuracies resulted from the transformation procedure described at the end of the subsection 2.2. The results presented in Fig.7 confirmed that the presented approach could not be used for the estimation of cracks depths (cf. Fig.6 and Fig.7 with Table 1). This is because of specific geometry of the particular cracks and the wavelet selected for the analysis, which results in different magnitudes of D -coefficients and have no practical background. In several cases (see e.g. Fig.7 for the case 25) the cracks were not identified, therefore the cracks detection and localization procedures should be carried out for the beams under the multiple stages of loading.

4. CONCLUSIONS

The new approach of cracks detection and localization in composite beams based on the image processing and wavelet analysis was presented. The results obtained during this study reveal the great precision of detection and localization of cracks even for the cases with considerably small damages. The application of the optimized fractional B-spline wavelet for the analysis allows for increase of the detectability and precision of the cracks localization. The main advantage of the presented approach is a possibility of its application in the conditions, where the direct contact measurements are not possible.

8. Morlier J., Salom P., Bos F.: New image processing tools for structural dynamic monitoring. "Key Engineering Materials" 2007, Vol. 347, p. 239 - 244.
9. Uhl T., Kohut P., Holak K., Krupiński K.: Vision based condition assessment of structures. "Journal of Physics: Conference Series" 2011, Vol. 305, No. 012043.
10. Patsias S., Staszewski W.J.: Damage detection using optical measurements and wavelets. "Structural Health Monitoring" 2002, 1, Vol. 1, p. 5 - 22.
11. Poudel U.P., Fu G., Ye J.: Structural damage detection using digital video imaging technique and wavelet transformation. "Journal of Sound and Vibration, 4-5, Vol. 286, p. 869 - 895.
12. Pakrashi V., O'Connor A.J., Basu B.: Damage calibration of a beam using wavelet analysis and image processing. "Bridge Engineering Research in Ireland", Third Symposium on Bridge and Infrastructure Research in Ireland, Dublin 2006.
13. Pakrashi V., Basu B., O'Connor A.J.: Structural damage detection and calibration using a wavelet-kurtosis technique. "Engineering Structures" 2007, Vol. 29, p. 2097 - 2108.
14. Katunin A.: Identification of multiple cracks in composite beams using discrete wavelet transform. "Scientific Problems of Machines Operation and Maintenance" 2010, 2, Vol. 45, p. 41 - 52.
15. Katunin A.: The construction of high-order B-spline wavelets and their decomposition relations for fault detection and localisation in composite beams. "Scientific Problems of Machines Operation and Maintenance" 2011, 3, Vol. 46, p. 43 - 59.
16. Katunin A.: Crack identification in composite beam using causal B-spline wavelets of fractional order. "Modelowanie Inżynierskie" 2013, No. 46, Vol. 15, p. 57 - 63.
17. Rucka M., Wilde K.: Crack identification using wavelets on experimental static deflection profiles. "Engineering Structures" 2006, Vol. 28, p. 279 - 288.
18. Katunin A., Gnatowski A.: Influence of the heating rate on evolution of dynamic properties of polymeric laminates. "Plastics, Rubber and Composites" 2012, Vol. 41, p. 233 - 239.
19. Timoshenko S., Woinowsky-Kreiger S.: Theory of plates and shells. 2nd ed., New York-Toronto-London 1959.
20. Luisier F., Blu T., Forster B. Unser M.: Which wavelet bases are the best for image denoising? Proceedings of the SPIE Conference on Mathematical Imaging "Wavelet XI", San Diego CA, USA, 2005.
21. Unser M., Blu T.: Fractional splines and wavelets. "SIAM Review" 2000, 1, Vol. 42, p. 43 - 67.
22. Van de Ville D., Unser M.: Complex wavelet bases, steerability, and the Marr-like pyramid. "IEEE Transactions on Image Processing" 2008, 11, Vol. 17, p. 2063 - 2080.
23. Chaudhury K.N., Unser M.: Construction of Hilbert transform pairs of wavelet bases and Gabor-like transforms. "IEEE Transactions on Signal Processing" 2009, 9, Vol. 57, p. 3411 - 3425.
24. Blu T., Unser M.: A complete family of scaling functions: the (,)-fractional splines. Proceedings of IEEE International Conference on Acoustics, Speech, and Signal Processing" 2003, Vol. 6, p. 421 - 424.